Supporting information for Photonic and plasmonic guided modes in graphene-silicon photonic crystals

Tingyi Gu[1,2 ‡], Andrei Andryieuski[3‡], Yufeng Hao[4], Yilei Li[5,6], James Hone[4], Chee Wei Wong[4,7], Andrei Lavrinenko[3], Tony Low[1,8*‖] and Tony F. Heinz[1,5]

[1] Department of Electrical Engineering, Columbia University, New York, NY 10027

[2] Princeton University, Princeton, NJ 08544

[3] DTU Fotonik, DTU, Oersteds pl. 343, Kongens Lyngby, Denmark 2800

[4] Department of Mechanical Engineering, Columbia University, New York, NY 10027

[5] Department of Physics, Columbia University, New York, NY 10027

[6] Department of Applied Physics, Stanford University, Stanford, CA 10027

[7] Mesoscopic Optics and Quantum Electronics Laboratory, University of California Los Angeles, CA 90095

[8] Department of Electrical and Computer Engineering, University of Minnesota, Minneapolis, MN 55455, USA

List of contents:

S1. Theoretical

S1.1. Simulated materials and structures

S1.2 Graphene plasmons

S1.3. Graphene covered 1D silicon subwavelength grating

S2. <u>Experimental</u>

S2.1 Raman characterization of graphene-on-photonic crystal structure

S2.2 Effective index calculation and reflectivity of multilayer structure

S2.3 Fano fit to the substrate guiding modes in near IR region

S1. Theoretical

S1.1. Simulated materials and structures

The simulated structure (Figure S1) corresponds to the fabricated one. Refractive indices of silicon[1] and silica[2] are shown in Figure S2a-b, respectively. Graphene's conductivity in the random phase approximation can be calculated [3] as

$$\sigma_S(\omega) = \frac{2e^2 k_B T}{\pi\hbar^2} \ln\left[2\cosh\left(\frac{E_F}{2k_B T}\right)\right] \frac{i}{\omega + i\gamma} + \frac{e^2}{4\hbar}\left[H\left(\frac{\omega}{2}\right) + \frac{4i\omega}{\pi}\int_0^\infty dx \frac{H(x) - H\left(\frac{\omega}{2}\right)}{\omega^2 - 4x^2}\right], \quad \text{(S2)}$$

where e is elementary charge; k_B is Boltzmann's constant; T is absolute temperature; $\hbar$ Planck's constant; γ damping rate and $H(x)$ is defined as:

$$H(x) = \frac{\sinh\frac{\hbar x}{k_B T}}{\cosh\frac{E_F}{k_B T} + \cosh\frac{\hbar x}{k_B T}} = \frac{1}{2}\left[\tanh\left(\frac{\hbar x + E_F}{2k_B T}\right) + \tanh\left(\frac{\hbar x - E_F}{2k_B T}\right)\right] \quad \text{(S3)}$$

Graphene's conductivity for $E_F = 0.3$ eV, $\gamma = 2 \times 10^{13}$ s^{-1} and $T = 300$ K is shown in Figure 2c. If the interband contribution to the conductivity is negligible, that is the case for $\hbar\omega < 2E_F$ and the electrochemical potential is larger than thermal fluctuation energy $E_F > k_B T$, graphene's conductivity can be described with Drude formula

$$\sigma_S(\omega) = \frac{e^2 E_F}{\pi\hbar^2}\frac{i}{\omega + i\gamma} \quad \text{(S4)}$$

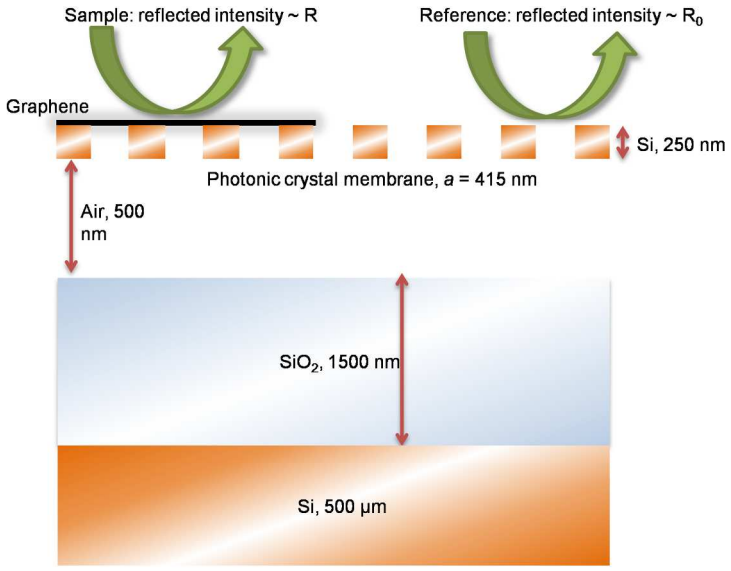

Figure S1. Simulated structure consists of a silicon photonic crystal membrane (thickness d = 250 nm, lattice constant a = 415 nm) suspended above silica (1.5 µm) on silicon substrate.

We restored the effective index of the suspended photonic crystal membrane from reflection and transmission simulation[4]. The effective index decrease with hole radii increase due a decreasing silicon filling fraction. A kink in the spectra shifting from 6000 to 7000 cm^{-1} corresponds to the first Fabry-Perot resonance condition $d = \lambda_0/2n_{eff}$.

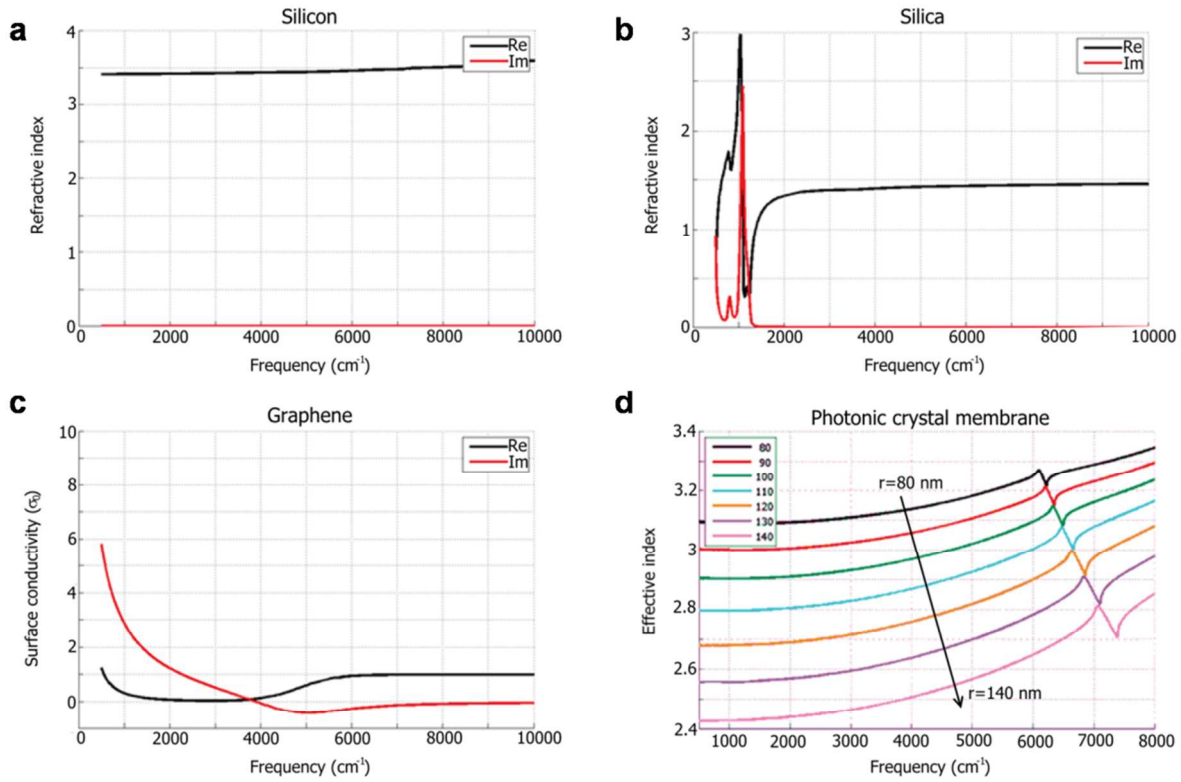

Figure S2. Effective index of the photonic crystal membrane depending on holes radii. The refractive index of silicon and silicon are given in ref. 1 and ref. 2 respectively. surface conductivity of graphene in units of $\sigma_0 = e^2/4\hbar$ ($E_F = 0.3$ eV, $\gamma = 2 \times 10^{13}$ s^{-1}, $T = 300$ K). Simulations were done in CST Microwave Studio[5] with time-domain solver, rectangular mesh and effectively periodic (x-axis perfect electric conductor, y-axis perfect magnetic conductor, z-open) boundary conditions. Fine spatial discretization was needed for consistent results (for example, 1 nm thick graphene layer was discretized with the step of 0.1 nm). Typical time for one simulation was 6 hours on 12 CPUs (3 GHz), 48 GB RAM computer.

S1.2 Graphene plasmons

Dispersion of transverse magnetic (TM) plasmons in graphene layer placed between two dielectrics with the permittivities $\varepsilon_1$and ε_2 is described by the dispersion equation[6]

$$\frac{\varepsilon_1}{\sqrt{q^2(\omega)-\varepsilon_1}} + \frac{\varepsilon_2}{\sqrt{q^2(\omega)-\varepsilon_2}} + i\sigma_S(\omega)Z_0 = 0 \qquad \text{(S1)}$$

where $q = \beta/k_0$ is the normalized propagation constant or in other words effective mode index (β is the propagation constant and $k_0 = \omega/c$ is the wavenumber in vacuum), σ_S is the surface conductivity of graphene and $Z_0 = \sqrt{\mu_0/\varepsilon_0} = 1/c\varepsilon_0 = 120\pi[\Omega]$ is the free-space impedance.

Taking into account graphene's plasmons' large effective index $q \gg 1$ and typical dielectrics have permittivity in the range of 1-12, the dispersion relation can be simplified as:

$$q(\omega) = \frac{(\varepsilon_1+\varepsilon_2)\pi\hbar^2}{Z_0 e^2 E_F}(\omega + i\gamma) \tag{S5}$$

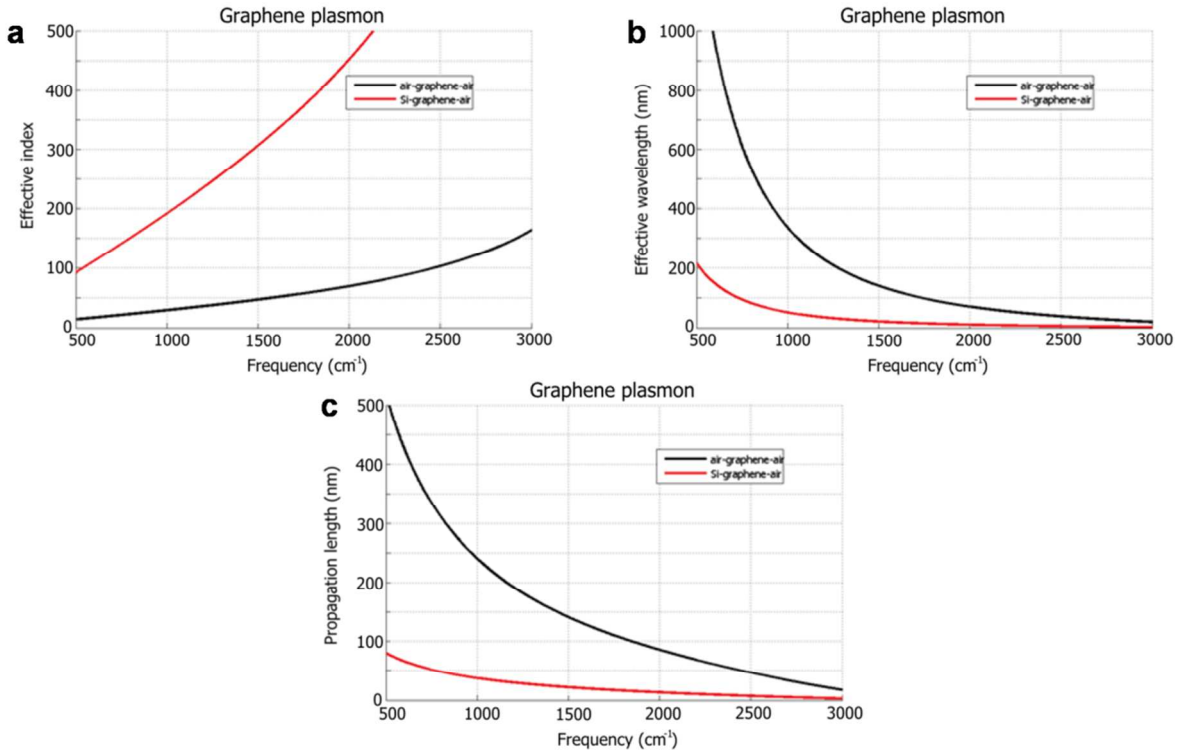

Figure S3. Effective index (a), effective wavelength (b) and propagation length (c) of plasmons in graphene suspended in air (black line) or supported on silicon (red line). Graphene's electrochemical potential is $E_F = 0.3$ eV and damping rate $\gamma = 2 \times 10^{13}$ s^{-1}.

Propagation constant (see the effective mode index for $E_F = 0.3$ eV and $\gamma = 2 \times 10^{13}$ s^{-1} in Figure S3a) depends on the graphene's surrounding and thus the plasmons propagating on suspended graphene and

graphene on silicon have different speed (effective index), thus forming plasmonic crystal or metamaterial (another way to form it is to structure graphene [7]). Typical plasmon wavelength (Figure S3b) as well as propagation length (Figure S3c) range from a few tens to a few hundreds nanometers in the frequency range of interest (500-3000 cm^{-1}).

S1.3. Graphene covered 1D silicon subwavelength grating

For a better understanding of the photonic and plasmonic regimes we simulated graphene on a simplified one-dimensional photonic crystal (see Figure S4) with a period a, thickness t and air hole width w. The absorbance spectrum revealed a bunch of resonances. For a fixed period a = 100 nm and increasing air filling fraction w/a (Figure S4a) we observe reduction of number of silicon-graphene-air resonances and their blueshift that is consistent with the previously observed excitation of the plasmons on supported part (with decreasing silicon size the resonator length decreases thus the resonant frequencies increase). Meanwhile the air-graphene-air plasmonic modes redshift (Figure S4a).

For the fixed w/a ratio and increasing grating period a (Figure S4b) there is observed a red-shift (resonator size becomes larger) with a trend resonance broadening. For the period a = 500 nm we can hardly distinguish more than one resonant peak whereas at a = 100 nm there are many. The reason for this is clear if we remember the typical propagation length for the supported graphene plasmons (see above) are less than 100 nm. For the resonator size of several hundreds of nm a plasmon excited at the edge of silicon decays before reaching the opposite side of the resonator, thus the resonance cannot be formed (in other words, the quality factor of the resonator is very low).

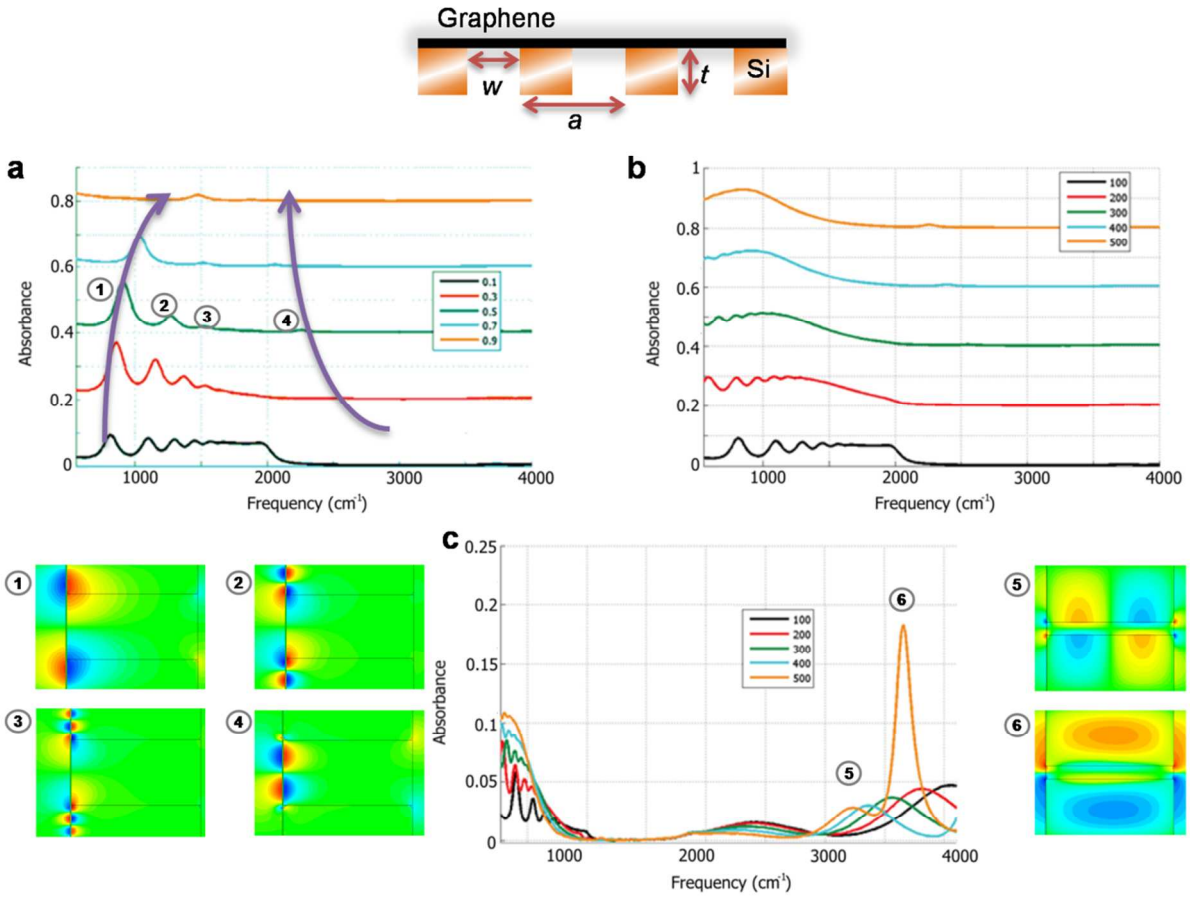

Figure S4. Simplified 1D photonic crystal consisting of silicon subwavelength grating and graphene (E_F = 0.3 eV) in air. (a) Absorbance for a = 100 nm, t = 100 nm and varying w/a = 0.1- 0.9. Silicon-graphene-air plasmonic modes (insets 1-3) exhibits blue shift and reduction of number of modes with increasing w/a, whereas air-graphene-air mode redshifts (inset 4). (b) Absorbance for w/a = 0.1, t = 100 nm and varying period a = 100 – 500 nm. Silicon-graphene-air modes redshift and broaden with period a increase. (c) Absorbance for a thick membrane t= 500 nm, w/a = 0.1 and varying period a = 100 – 500 nm. Plasmonic modes exhibit a similar behavior to the case (b) in the low frequnecies, whereas in the high frequencies photonic modes (insets 5 and 6) are observed.

In the previous cases (Figure S4a-b) the silicon membrane was assumed t = 100 nm thick. In low frequencies, in principle, there are no principal differences between thick and thin membranes (as soon as the membrane is still subwavelength). Small thickness does not allow for photonic modes excitation and guiding. If we increase the thickness to t = 500 nm plasmonic modes exhibit qualitatively the same behavior in the low frequencies, while in the high

frequencies absorbance peaks corresponding to photonic modes appear (Figure S4c). The electric fields at resonant frequencies represent the whole "zoo" of possible excitations (Figure S4, insets 1-6), including silicon-graphene-air and air-graphene-air plasmonic and silicon grating photonic modes.

S2. Experimental

S2.1 Raman characterization of graphene-on-photonic crystal structure

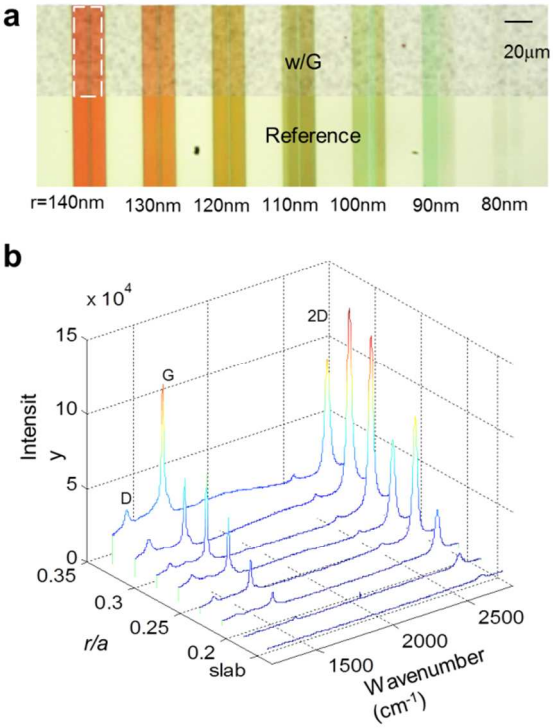

Figure S5. (a) Optical microscope image of device layout, with strips of silicon superlattice with hole radius r decreasing from 140 to 80 nm in step of 10 nm (left to right). Graphene covers the shadowed area on top. The dashed square marks the region of FTIR window. (b) Raman spectrum for graphene superlattice with different radius versus lattice constant ratio r/a.

S2.2 Effective index calculation and reflectivity of multilayer structure

The suspended porous silicon thin film is 250nm thick (d) with silicon filling factor (δ) of 64%~88% as the hole radius increasing from 80nm to 140nm. The effective refractive index of the porous silicon thin film can be derived from the Maxwell-Garnett equation:

$$n_{eff} = \sqrt{\frac{2(1-\delta)n_{air}^{\ 2} + (1+2\delta)n_{Si}^{\ 2}}{(2+\delta)n_{air}^{\ 2} + (1-\delta)n_{Si}^{\ 2}}} \tag{S6}$$

where the refractive index of silicon n_{si}=3.42 in IR range. Transfer-matrix method is then applied to derive reflectance (r) for electromagnetic field normally incident onto the porous silicon thin film with effective wavenumber $k_{eff} = 2\pi n_{eff}/\omega$, suspended in air (with vacuum wavenumber k_0)[8]:

$$r = \frac{-k_{eff}\sin k_{eff}d + (k_0^{\ 2}/k_{eff})\sin k_{eff}d}{k_{eff}\sin k_{eff}d + (k_0^{\ 2}/k_{eff})\sin k_{eff}d + i2k_0\cos(k_{eff}d)} \tag{S7}$$

The reflection spectrum ($R = |r^2|$) superimposed on the incident thermal source spectrum can be directly measured (Figure S6a), and compared to the simulated reflectance (inset of Figure S6a). The single atomic layer graphene exerts little modification on the absolute reflection spectrum (red solid curve in Figure S6a) compared to the substrate (grey dashed curve). The broadband reflection spectrum with controlled hole radius can be well described by the Transfer-matrix method (Figure S6b).

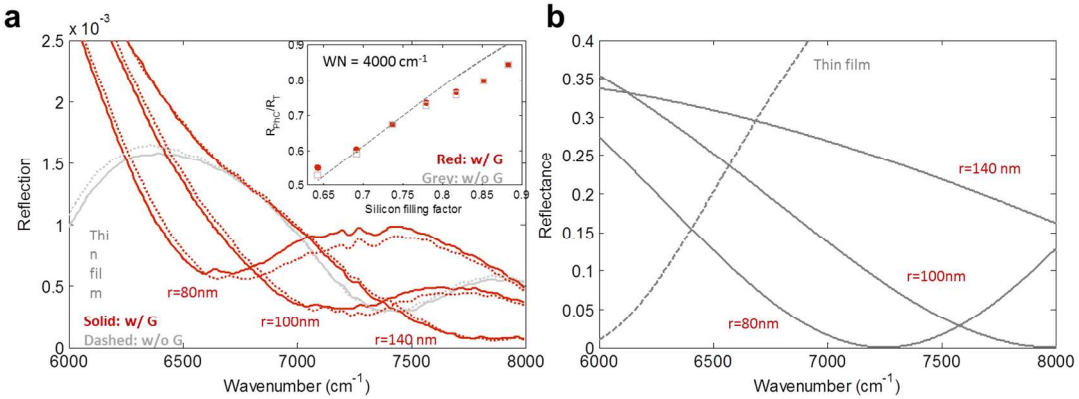

Figure S6. Measured reflection spectrum for graphene-silicon superlattice. (a) Absolute reflection spectrum of 250nm silicon thin film and photonic crystals with hole radius increasing

from 80-140 nm, in step of 10nm (from top to bottom), with (red solid curve) and without (grey dashed curve) coverage. Inset: reflected signal at 4000cm-1 wavenumber normalized by the thin film silicon. Red solid circles/grey empty squares: with/without graphene coverage. The dashed line is from simulation as shown in b. (b) Calculated reflection spectrum as shown in (a).

S2.3 Fano fit to the substrate guiding modes in near IR region

The extinction spectrum in the reflection, 1-R/R_0, can be fitted by Fano resonance lineshape to experiments[9,10] (Figure S7a):

$$1 - R / R_0 = A \frac{\left(q + \frac{\omega - \omega_0}{\Gamma / 2} \right)^2 + b}{1 + \left(\frac{\omega - \omega_0}{\Gamma / 2} \right)^2} \quad (1)$$

Where Γ_0 is the resonance frequency of the substrate guiding mode, and can be deterministically shifted by the substrate parameter; q is the asymmetry parameter, and fitted to be around -3. b is the screening parameter. A is amplitude of the resonance. A and b dependence on substrate parameter are fitted. The screening parameter b also limits the resonance width, Γ, which is the main effect of intrinsic losses in Fano resonances. The inverse of spectral width is the lifetime of the resonator, and fitted to be 0.1ps throughout the measurements in Figure S7b. At higher or lower loss rate, the Fano lineshape would have broader/narrow spectrum (Figure S7c), with fixed A=8%, b=-3. The screening parameter b (≈3) determines the contrast of the Fano lineshape (Figure S7d).

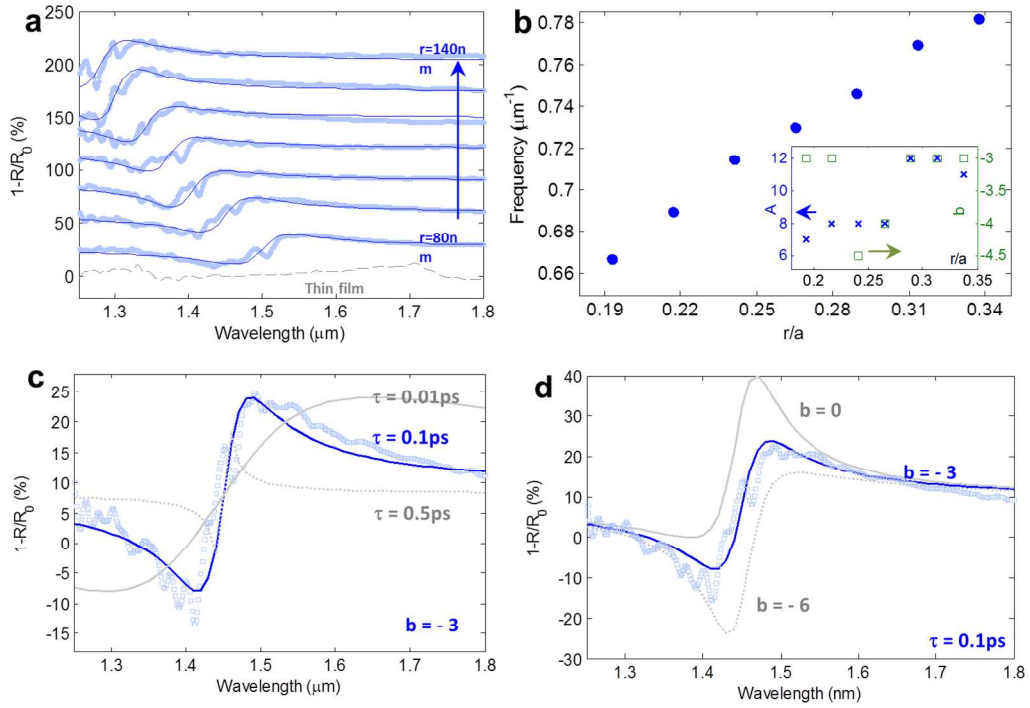

Figure S7. Graphene extinction spectrum coupling with photonic crystal guided resonance in near IR range. (a) Measured extinction spectra of graphene covered on 250nm thin film (grey dashed curve) and photonic crystals with fixed lattice constant and increasing hole radius (light blue dots). Solid blue curves are Fano resoannce curve fitting. Vertical cumulative offest of 30% is added for clarity. Inset: Amplitude of Fano resonance versus r/a. (b) Guiding mode resonance frequency versus radius versus lattice constant ratio as extracted from the curve fitting in a. (c) Comparison of measured extinction spectrum (blue empty squares r=90nm) with the Fano spectrum with different lifetimes and (d) screening parameters.

REFERENCES

(1) Palik, E. D.; Ghosh, G. *Handbook of optical constants of solids*; Academic press, 1998.

(2) Kitamura, R.; Pilon, L.; Jonasz, M. *Appl. Opt.* **2007**, *46*, 8118.

(3) Mason, D. R.; Menabde, S. G.; Park, N. *Opt. Express* **2014**, *22*, 847.

(4) Smith, D. R.; Schultz, S. *Phys. Rev. B* **2002**, *65*, 195104.

(5) CST. Computer Simulation Technology, AS http://cst.com.

(6) Jablan, M.; Buljan, H.; Soljačić, M. *Phys. Rev. B* **2009**, *80*, 245435.

(7) Yeung, K. Y. M.; Chee, J.; Yoon, H.; Song, Y.; Kong, J.; Ham, D. *Nano Lett.* **2014**, *14*, 2479–2484.

(8) Born, M.; Wolf, E.; Bhatia, A. B. *Principles of optics*; Pergamon Pr., 1970; Vol. 10.

(9) Ott, C.; Kaldun, A.; Raith, P.; Meyer, K.; Laux, M. *Science (80-.).* **2013**, *340*, 716–720.

(10) Gallinet, B.; Martin, O. J. F. *Phys. Rev. B* **2011**, *83*, 235427.

This information is available free of charge via the Internet at http://pubs.acs.org/photonics.